IEEE Transactions on Nuclear Science, Vol.NS-24, No.3, June 1977

RECENT RESULTS OF THE UNIVERSITY OF MARYLAND RESEARCH PROGRAM ON COLLECTIVE ION ACCELERATORS*

W. W. Destler, D. W. Hudgings, H. Kim, M. Reiser,
M. J. Rhee, C. D. Striffler, and G. T. Zorn
University of Maryland
College Park, Maryland 20742

Summary

Two collective ion acceleration schemes are being studied at the University of Maryland: (a) the electron ring method (ERA) and (b) collective acceleration with linear beams. In the ERA, a hollow, axially moving ($\beta_z \approx 0.2$) electron beam is formed by the cusp method. This beam is to be stopped for ion loading by resistive wall interaction and a fast magnetic mirror system. The rings are then accelerated by the magnetic expansion method over a distance of 1.4 m. During stopping experiments with resistive walls, a rapid growth of the radial beam width was observed which led to severe particle loss. This effect is attributed to radial off-centering in the cusp, mismatch in the equilibrium radius due to self fields, and the negative mass instability. It can be suppressed by the use of cusp correction coils, proper boundaries and Landau damping with scattering foils. In the linear-beam experiment, proton beams of 16 MeV energy, peak currents of 10 kA, pulse length of 3 ns, focused to 1 cm diameter have been obtained. Slow-wave structures to increase the ion energy are studied.

Electron Ring Accelerator Studies

In fall 1975, 14 magnet coils, a new vacuum chamber with a long "squirrel cage" inner conductor, and a vacuum pump assembly were added to the existing ERA facility downstream from the cusp iron plate. A schematic of the completed system and the shape of the axial magnetic field is shown in Fig. 1. The new field geometry provides a gradient dB_z/dr over a distance of 140 cm for ring acceleration by the expansion method. It also allows the study of the propagation and characteristics of the downstream beam over a larger distance and time span than was possible previously in the much shorter 7-coil field geometry.

Fig. 2 illustrates the concept of ring formation, ion loading, and acceleration in our ERA experiment.[1] Fig. 2(a) represents the present phase of the experiment. The rotating beam emerging from the cusp has a minimum axial velocity in the range of $\beta_z = 0.2$ to 0.3 and, at this stage, resembles a short "E-layer" with axial dimensions comparable to the diameter (2R=12 cm). Fig. 2(b) shows the next phase when the beam will be stopped at about $z = 50$ cm by interaction with a resistive wall[2] and/or the gas cloud[3] from the puff valve. A fast-pulse coil system will be added to trap and load the ring with ions under more controllable conditions. The axial dimensions of the beam will be reduced as β_z goes to zero. Fig. 2(c) shows the axial variation of the main magnetic field, the small mirror that results when both trapping coils are on, and the variation of the axial ring velocity β_z with distance z. At the point $\beta_z \approx 0$, ions are trapped in the ring and the subsequent acceleration then depends on the holding power, number of ions in the ring, and the total distance traveled. The "squirrel cage" conductor inside the beam suppresses azimuthal image currents and thereby provides axial focusing of the ring beam.

After completion of the extended coil system, we started experiments to stop the electron beam with the resistive-wall method (the resistive layer, 20 Ω per square, was mounted on the squirrel cage). During these experiments, a rapid growth of the radial beam width was observed which occurred both with and without the presence of the resistive layer and resulted in a severe beam loss to both inner and outer conductors. We then started a systematic experimental and theoretical program aimed at a full understanding of this effect and at finding ways by which it could be suppressed.

The major results of the experimental studies that have been done so far are presented in a separate paper.[4]

From these experimental data, one can obtain a qualitative picture of the deterioration of the beam quality if one divides the number of electrons N by the major radius R and the minor beam dimensions $(\Delta R + \Delta z)$ as a function of distance z of beam propagation in the downstream magnetic field. This crude "figure of merit" can also be expressed as an average electric field at the surface of the beam:

$$E_{av}\left[\frac{MV}{m}\right] = \frac{18.4 \times 10^{-12}\,N}{R[cm]\,(\Delta R + \Delta z)\,[cm]}\,,$$

which is not identical with the "holding power" for the ions since boundary effects are neglected. Fig. 3 shows a plot of E_{av} versus z for an electron beam intensity of $N = 5 \times 10^{13}$ (corresponding to an injected beam current of about 4 kA) in two drift-tube geometries. It should be noted that the electron energy is 2.5 MeV; the radii of inner and outer walls are 4.5 and 7.5 cm and the beam is injected with a radius of 6.0 cm. The focusing effect of the inner squirrel cage results in a shorter axial length and thus higher initial particle density. But, as the figure illustrates, the radial blowup then quickly destroys the beam quality and at $z = 75$ cm, E_{av} is actually lower than in the case with no inner squirrel cage. Fig. 4a is a time-integrated photograph of the beam when it hits a Plexiglas stop at $z = 100$ cm (in a case where only a solid outer conductor was present). The severe deterioration of the beam quality is obvious. It was also observed in these experiments that the radial blowup effect is accompanied by intense microwave radiation in X-band (8-12 GHz) and KA-band (26-40 GHz) which increases rapidly with intensity. The most important experimental result, however, is the fact that beam deterioration and microwave radiation can be drastically reduced by passing the beam through a thin titanium foil (6.3 mg/cm^2). This is illustrated in Fig. 4b which shows the time-integrated photograph of the beam when such a foil is used.

Our present understanding is that the observed radial blowup effect is due to a combination of negative mass instability, mismatch of radial force equilibrium due to self field (particularly when an inner squirrel cage is present), and an increase of radial width due to single-particle off-centering in the transition through the magnetic cusp (slit in iron plage). In the following, we discuss these three effects and the results of theoretical studies.

Single-particle effects in the cusp. The coherent off-centering experienced by the electron when they pass through the cusp is illustrated in Fig. 5, which also shows (schematically) the variation of magnetic field components B_z and B_r versus z at the mean radius of R = 6 cm. In a first-order theory, Rhee and Destler[5] found for the coherent radial width, $\Delta R_{coh} = R_{max} - R_{min}$, the approximate expression

$$\Delta R_{coh} = \lambda \sin^{-1} (R\omega_c/v) \ , \qquad (1)$$

where the magnetic field is represented by $B_z = -B_o \tanh z/\lambda$, and ω_c is the electron cyclotron frequency. In our cusp field $\lambda \approx 1$ cm, which yields $\Delta R_{coh} = 1$ cm when $v_\Theta = R\omega_c = v$, in agreement with experimental results. One way of decreasing ΔR_{coh} is to reduce the cusp width. Another way is to compensate the outward radial force in the cusp by an inward force. This is essentially accomplished by adding a short bump ΔB_z to the uniform field B_o upstream from the cusp transition, as shown in Fig. 5 (dotted line). One can show that in first-order approximation, the bump field required to balance the coherent off-centering effect is given by

$$2 \int_{z_1}^{z_2} (\Delta B_z/B_o) dz = \Delta R_{coh} \ . \qquad (2)$$

To investigate theoretically the possibility of reducing the off-centering with correction coils, we solved numerically the relativistic single-particle equations of motion in an analytical magnetic field that is a very close approximation of the actual field configuration. In these studies,[6] two correction coils were placed on either side of the iron plate. These coils sharpen the cusp width (parameter λ) and, in addition, the upstream coil provides a bump ΔB_z that compensates for the coherent off-centering that the particles still experience when traversing the narrower cusp. Based on these numerical studies, a two-coil correction system was designed which has been completed and will be tested shortly in the ERA facility.

Radial beam equilibrium. The equilibrium state of a rotating long E-layer moving with axial velocity v_z was examined theoretically[6] for geometry I (outer conductor only) and geometry II (outer conductor and inner squirrel cage) of our ERA experiment. The electrons all have the same canonical angular momentum p_Θ (defined by the magnetic flux linking the cathode) and the same total energy $\gamma_a m_o c^2$ after acceleration in the diode. In the equilibrium state downstream from the cusp iron plate, we have an electric self field $E_r = -\partial\phi/\partial r$ and magnetic self field components B_z, B_Θ. The applied magnetic field B_o outside the cusp region is assumed to be uniform. Let R_I be the cathode radius, R the equilibrium radius of the downstream beam. We then have the following equations:

$$\gamma(R) = \gamma_a + \frac{e}{m_o c^2} \phi(R) \quad \text{(total energy)} \qquad (3)$$

$$v_\Theta(R) = -\frac{e}{2m_o\gamma} \frac{R_I^2 B_o + R^2(B_o - B_z)}{R} \quad (\text{from } p_\Theta = \text{const}) \qquad (4)$$

$$\frac{m_o \gamma v_\Theta^2}{R} = eE_r(R) - ev_\Theta[B_o - B_z(R)] - ev_z B_\Theta(R) \qquad (5)$$

(radial force balance)

The self fields are proportional to the axial beam current and can be determined in a straightforward way (since $\partial/\partial z = 0$, $\partial/\partial\Theta = 0$) for the two geometries. The equilibrium radius R was calculated for different beam currents I and field levels B_o. In geometry I, R is found to be greater than the injection radius ($R > R_I$) and increases as the current I gets larger or as v_z decreases. For geometry II, we find $R < R_I$, i.e., the beam radius shrinks with increasing I and decreasing v_z and the beam gets lost to the squirrel cage (R = 4.5 cm) when I gets too large or v_z too small. For a given current I and axial velocity v_z, the change in radius R is more pronounced in the squirrel-cage geometry than in case I. Further studies are now in progress to determine better equilibrium conditions by changing the boundaries and unbalancing the cusp field.

Negative mass instability. The existing theory of negative mass instability is for stationary ring beams. The stability criterion derived from the dispersion relation for the cavity modes states that the total number of particles in the ring must be less than a critical number N_{max} given by[7]

$$N_{max} = \frac{\gamma R}{2\beta^3 r_e} \frac{Z_o}{|Z_\ell/\ell|} \left(\frac{\Delta E}{E}\right)^2 \left(\frac{1}{\nu_r^2} - \frac{1}{\gamma^2}\right), \qquad (6)$$

where r_e is the classical electron particle radius, Z_ℓ the coupling impedance for the ℓ-th mode, ν_r the betatron time and $(\Delta E/E)$ the energy spread in the beam. Recently, Uhm and Davidson[8] have extended this theory to a long stationary E-layer beam and obtained a similar dispersion relation for the number of electrons per unit length. Neither model represents the short moving E-layer in our present phase of the ERA experiment. However, the general conclusions from both models are applicable to our beams, namely, (a) that there exists an intensity threshold which depends on the energy spread (or, more accurately, the spread in canonical angular momentum, Δp_Θ) and the boundary conditions, and (b) that, in the case where the beam is unstable ($N > N_{max}$), the growth rate increases as the number of particles in the beam gets larger. The results in geometry I (outer conductor only), where most of the data was taken, appear to indicate that without a scattering foil we are not too far above the threshold. The titanium foil has two effects: It introduces a relatively small amount of angular scattering and energy dispersion ($\Delta E/E < 1\%$) and, according to the experimental observations, reduces the sharp density peak at the beam-front. Lower particle density combined with Landau damping then significantly reduces the growth rate of the instability or even suppresses it entirely. The present observation time of the moving beam is still too short to determine whether, and at which intensity level, the instability is fully eliminated. To decide this question, we have to wait for the stopping experiments when the electron ring is trapped for ion loading and can be observed over a longer time period. Further studies, both experimentally as well as theoretically, are required to determine the optimum combination of intensity, boundary conditions, and scattering foil that yields the best beam quality and holding power for collective ion acceleration by the ERA method.

Linear-Beam Collective Ion Acceleration Studies

By changing the cathode-anode geometry of our ERA injector, we can generate straight cylindrical beams with energies in the 1 MeV range, currents of 20-40 kA, and pulse lengths of 30-40 ns. With these beams, we are studying collective-ion acceleration in vacuum. This method, pioneered by Luce and collaborators at Livermore,[9] has so far yielded the highest energy amplification factors. The most recent results of our work in this rather promising area are presented in a separate paper at this conference.[10] Protons have been accelerated to peak energies of at least 16 MeV with peak currents as high as 12 kA. The protons are concentrated in a rather short, well-defined bunch less than 5 ns long and can be focused to less than 1 cm diameter by a relatively low magnetic field of 1.8 kG. We have also accelerated carbon ions to energies above 20 MeV. The great potential of this type of collective-field accelerator as a combination of heavy ion source and injector for a pellet-fusion accelerator is discussed in another conference paper.[11] Available data indicates that one should get heavy-ion beams with energies of order 1 MeV per nucleon and currents of order 10^2 to 10^3 amperes. The basic physical mechanisms in this acceleration method are not yet fully understood. The ions are created in a plasma at the anode aperture through which the electron beam passes into the vacuum region and are accelerated by the space charge field. Our main effort at present is aimed at better understanding of the beam characteristics, improving the diagnostics, acceleration of heavy ions, and increasing the ion energy by use of slow-wave structures.[10] The product of average kinetic energy and total number of ions is limited by the total energy contained in the electron beam. We found that the peak proton energy increases proportionally to the electron beam power. With respect to heavy ions, one expects that the energy per nucleon will decrease with mass number as has been observed. Further studies are needed to determine the energy conversion efficiency from electron to ion beam and the scaling laws with regard to ion mass, intensity, and peak energy.

References

1. M. Reiser, IEEE Trans. NS-20, 310 (1973); Destler et al., Proc. IXth Int. Conf. on High Energy Accelerators, Stanford, 1974, p. 230.
2. J.G. Kalnins et al., IEEE Trans. NS-20, 324 (1973); P. Merkel, Particle Accelerators 7, 69 (1976).
3. U. Schumacher et al., Part. Accel. 7, 245 (1976).
4. W.W. Destler, D.W. Hudgings, M.J. Rhee, Paper J 15.
5. W.W. Destler, M.J. Rhee, Phys. Fluids 17, 1574 (1974).
6. C.D. Striffler et al., Phys. Tech. Repts. 77-063 and 77-062, Univ. of Maryland.
7. L.J. Laslett, IEEE Trans. NS-20, 271 (1973).
8. H.S. Uhm and R.C. Davidson, Physics Publ. 77-044, Univ. of Md., to be published in Phys. Fluids.
9. J.S. Luce et al., IEEE Trans. NS-20, 336 (1973).
10. C.N. Boyer, W.W. Destler, and H. Kim, Paper J 7.
11. M. Reiser, Paper B 11.

*Research supported by NSF Grant No. PHY7611178.

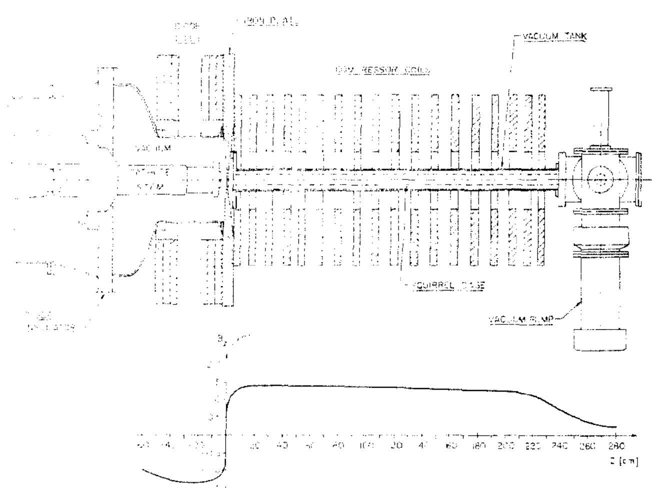

Fig. 1. Diode and coil system of ERA facility.

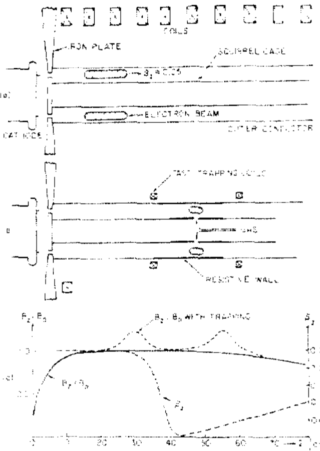

Fig. 2. Schematic of University of Maryland ERA scheme.

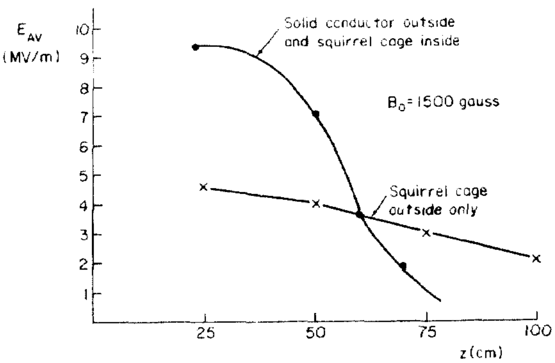

Fig. 3. E_{av} at beam surface versus distance z.

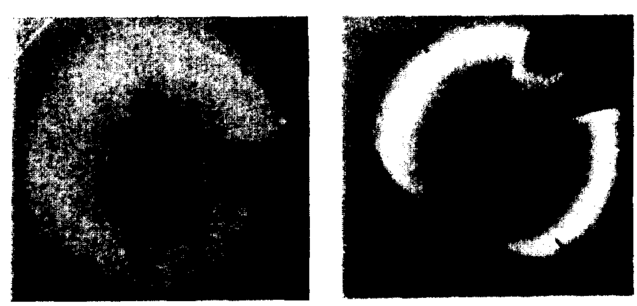

(a) (b)

Fig. 4. Beam cross section without (a) and with (b) foil.

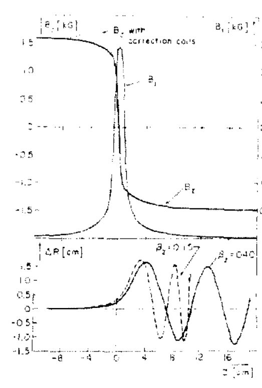

Fig. 5. Cusp field and coherent radial oscillations.